Available online at www.sciencedirect.com

ScienceDirect

Journal of Molecular Structure 825 (2006) 32–37

Journal of
MOLECULAR
STRUCTURE

www.elsevier.com/locate/molstruc

Bromodifluoroacetyl fluoride, $CF_2BrC(O)F$: Experimental and theoretical studies

Valeria B. Arce [a], Joanna Czarnowski [b], Rosana M. Romano [a,*]

[a] *CEQUINOR (CONICET, UNLP) Departamento de Química, Facultad de Ciencias Exactas, Universidad Nacional de La Plata, 47 y 115, 1900 La Plata, Argentina*

[b] *Instituto de Investigaciones Fisicoquímicas Teóricas y Aplicadas, INIFTA, Sucursal 4, Casilla de Correo 16, (1900) La Plata, Argentina*

Received 23 March 2006; received in revised form 4 April 2006; accepted 4 April 2006
Available online 24 May 2006

Abstract

Bromodifluoroacetyl fluoride, $CF_2BrC(O)F$, was prepared through the gas-phase reaction of bromotrifluoroethene, CF_2CFBr, with molecular oxygen initiated either by NO_2 or CF_3OF. The compound was experimentally studied by FTIR spectroscopy of the gas phase and also isolated in Ar and N_2 matrices at low temperature. The energy differences between the possible conformers were theoretically studied, as well as the vibrational spectra of the conformers.

Keywords: Conformational analysis; Matrix isolation; FTIR spectroscopy; Theoretical calculations; Bromodifluoroacetyl fluoride; Gas-phase reaction

1. Introduction

Several halodifluoroacetyl halides of the type $CF_2XC(O)Y$, with X, Y = halogen, have been subject of conformational and vibrational studies during the last years. $CF_2ClC(O)F$ [1], $CF_2ClC(O)Cl$ [2], and $CF_2BrC(O)Cl$ [3] have been found to present predominantly the *gauche* conformation in equilibrium with the less stable *anti* conformer (X atom oriented *anti* to Y atom). As far as we know, there is no report in the literature about the bromodifluoroacetyl fluoride, $CF_2BrC(O)F$.

Here we present the preparation of bromodifluoroacetyl fluoride, $CF_2BrC(O)F$, through the gas-phase reaction of bromotrifluoroethene, CF_2CFBr, with molecular oxygen initiated either by NO_2 or CF_3OF. The compound was experimentally studied by FTIR spectroscopy of the gas phase and also as isolated in an inert matrix environment at low temperature. Theoretical calculations were performed in order to determine the energy differences between the possible conformers and also to predict the vibrational spectra of these conformers and thus help in the correct assignment of the vibrational absorptions.

2. Experimental

The bromodifluoroacetyl fluoride, $CF_2BrC(O)F$, was produced as the main product of the thermal gas-phase oxidation of bromotrifluoroethene, CF_2CFBr, with molecular oxygen initiated either by the addition of NO_2 [4] or CF_3OF to the double bond of the alkene.

All reactants were purchased commercially. NO was eliminated from NO_2 (Matheson 99.5%) by a series of freeze–pump–thaw cycles in presence of O_2 until disappearance of the characteristic blue colour of N_2O_3. Finally, the degassed NO_2 was purified by fractional condensation using the fraction that distilled between 213 and 243 K. CF_3OF (PCR, 97–98%) was washed with 0.1 mol dm^{-3} NaOH and filtered at 80 K [5]. The CF_2CFBr (PCR, 97–98%) contained CF_4, and CF_3CF_3 as impurities. These impurities are more volatile than CF_2CFBr, but, as distilling together could not be separated by fractional condensation. The CF_2CFBr was purified by intermittent brief

---

[*] Corresponding author.
E-mail address: romano@quimica.unlp.edu.ar (R.M. Romano).

0022-2860/$ - see front matter © 2006 Elsevier B.V. All rights reserved.
doi:10.1016/j.molstruc.2006.04.011

evacuation cycles at 153 K, opening and closing the trap valve. This procedure was repeated several times, until the disappearance of the respective very strong absorption bands of CF_4 [6] and CF_3CF_3 [7] at 1279 and 1250 cm^{-1}, respectively, in the IR spectrum of CF_2CFBr. Oxygen (La Oxígena 99.99%) was bubbled through 98% analytical-grade H_2SO_4 and passed slowly through a Pyrex coil at 153 K.

The experiments were performed in a grease-free conventional static system, allowing pressure measurements at constant volume and temperature. A spherical quartz bulb of 270 cm [3] was used as reaction vessel. The pressure was measured with a quartz spiral gauge.

Infrared spectra of the reaction mixtures were recorded on Shimadzu IR-435 spectrometer. The gas and matrix-isolated FTIR spectra of $CF_2BrC(O)F$ were recorded on a Nexus Nicolet instrument equipped with either an MCTB or a DTGS detector (for the ranges 4000–400 or 600–200 cm^{-1}, respectively). The gas FTIR spectra were recorded at ambient temperature using 10 cm cell provided with KBr windows with a 0.5 cm^{-1} resolution.

Gas mixtures of $CF_2BrC(O)F$ with Ar and N_2 (both AGA) in the proportion ca. 1:1000, prepared by standard manometric methods, were deposited on a CsI window cooled to ca. 10 K by means of a Displex closed-cycle refrigerator (SHI-APD Cryogenics, Model DE-202) using the pulse deposition technique [8,9].

Following deposition and IR analysis of the resulting matrix, the sample was exposed to broad-band UV–visible radiation ($200 \leqslant \lambda \leqslant 800$ nm) from a Spectra-Physics Hg–Xe arc lamp operating at 1000 W. The output from the lamp was limited by a water filter to absorb IR radiation and so minimize any heating effects. The IR spectrum of the matrix with a 0.125 cm^{-1} resolution was then recorded at different times of irradiation in order to monitor closely any change in the spectra. The UV–visible spectra of the products in the gas phase were recorded on a Hewlett–Packard Model 8452A spectrometer, using a 10 cm quartz cell.

All of the quantum chemical calculations were performed using the Gaussian 98 [10] program system under the Linda parallel execution environment using two coupled PCs. Geometry optimizations were sought using standard gradient techniques by simultaneous relaxation of all the geometrical parameters. The calculated vibrational properties correspond in all cases to potential energy minima for which no imaginary vibrational frequency was found.

3. Preparation of bromodifluoroacetyl fluoride, $CF_2BrC(O)F$

3.1. Gas-phase reaction between NO_2, CF_2CFBr and O_2

The experiments were made at 313.4 K. The initial pressure of CF_2CFBr was varied between 18.8 and 43.9 Torr, that of NO_2 between 0.9 and 4.8 Torr and that of O_2 between 96.9 and 402.9 Torr. All experiments were carried out to the complete consumption of alkene. After all CF_2CFBr was consumed a slow pressure increase and the formation of Br_2 were observed.

The main reaction product was $CF_2BrC(O)F$. Its yields, based on the initial pressure of the alkene, increased from 79% to 85% as the pressure of NO_2 decreased from 4.8 to 0.9 Torr. Minor quantities of $C(O)F_2$ and C(O)FBr, and small amounts of $CF_2BrCFBrO_2NO_2$ and trifluorobromoethene epoxide (TFBrEO), 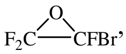 were also formed. The compounds $C(O)F_2$ [11] and C(O)FBr [12,13] were identified by their respective IR spectra. The formation of C(O)FBr was also detected by its UV spectrum in the range of 200–220 nm [13]. The product $CF_2BrCFBrO_2NO_2$ was identified by its infrared absorption band at 1758 cm^{-1}, characteristic to the NO_2 group of the haloalkylperoxynitrates and haloalkoxylperoxynitrate, appearing between 1754 and 1762 cm^{-1}. The trifluorobromoethene epoxide (TFBrEO), was identified in the reaction mixture by its infrared band at 1540 cm^{-1}, assigned to the ring-breathing mode, that is characteristic of fluoroepoxides. This band appears at 1500 cm^{-1} for 1,1-dichloro-2,2-difluoroethene epoxide [14], at 1550 cm^{-1} for chlorotrifluoroethene epoxide [14] and at 1551 cm^{-1} for perfluoropropene epoxide [15].

To obtain pure $CF_2BrC(O)F$, the reaction mixture in the reaction vessel was rapidly cooled to liquid air temperature and the mixture separated by fractional condensation. The fraction volatile between 158 and 183 K was $CF_2BrC(O)F$. The fractions of eight experiments were collected together to obtain major amount of bromodifluoroacetyl fluoride.

3.2. Gas-phase reaction between CF_3OF, F_2CFBr and O_2

The experiments were made at 273, 253.5 and 239 K. The initial pressure of CF_3OF was varied between 0.9 and 2.4 Torr, that of CF_2CFBr between 11.5 and 30.7 Torr and that of O_2 between 48.2 and 100.7 Torr.

At 273 K the reaction was completed in 10 min. At 253.5 and 239 K the time of permanence of the reaction system $CF_3OF + CF_2CFBr + O_2$ in the reaction vessel was between 42 and 121 min. In all runs the CF_2CFBr was completely consumed.

The main product was $CF_2BrC(O)F$ (yields 81–95% based on the CF_2CFBr consumed). Minor quantities of $C(O)F_2$ and C(O)FBr, and traces of $CF_3OCF_2C(O)F$ and bromotrifluoroethene epoxide 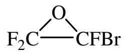 were also formed. $CF_3OCF_2C(O)F$ was identified by its IR spectrum [16].

The very strong absorption band of CF_3OOCF_3 at 1166 cm^{-1} [17] and that at 1122–1119 cm^{-1}, characteristic of $CF_3C(O)F$ [18], were not observed.

To determine the concentration of $CF_2BrC(O)F$, the room temperature infrared calibration curve was made, allowing conversion of the absorption intensities at 1887 cm^{-1} to the pressure of $CF_2BrC(O)F$. The pressure corresponding to the temperature of each run was calculated starting from the pressure of this compound at room temperature obtained from the calibration curve.

3.3. Mechanism postulated for the $CF_2BrC(O)F$ formation

The $CF_2BrC(O)F$ is formed through a chain reaction. The basic common chain reaction mechanism for the oxidation of CF_2CFBr, initiated by the addition of NO_2 or CF_3OF to the double bond of the olefin in presence of O_2, can be presumed to be as follows:

1. $NO_2 + CF_2CFBr \rightarrow O_2NCF_2CFBr^{\cdot}$
2. $CF_3OF + CF_2CFBr \rightarrow CF_3CFBr^{\cdot} + CF_3O^{\cdot}$
3. $CF_3O^{\cdot} + CF_2CFBr \rightarrow CF_3OCF_2CFBr^{\cdot}$
4. $O_2NCF_2CFBr^{\cdot} + O_2 + M \rightarrow O_2NCF_2CFBrO_2^{\cdot} + M$
5. $2O_2NCF_2CFBrO_2^{\cdot} \rightarrow 2O_2NCF_2CFBrO^{\cdot} + O_2$
6. $CF_3CFBr^{\cdot} + O_2 + M \rightarrow CF_3CFBrO_2^{\cdot} + M$
7. $2CF_3CFBrO_2^{\cdot} \rightarrow 2CF_3CFBrO^{\cdot} + O_2$
8. $CF_3OCF_2CFBr^{\cdot} + O_2 + M \rightarrow CF_3OCF_2CFBrO_2^{\cdot} + M$
9. $2CF_3OCF_2CFBrO_2^{\cdot} \rightarrow 2CF_3OCF_2CFBrO^{\cdot} + O_2$
10. $O_2NCF_2CFBrO^{\cdot} \rightarrow O_2NCF_2C(O)F + Br^{\cdot}$
11. $CF_3CFBrO^{\cdot} \rightarrow CF_3C(O)F + Br^{\cdot}$
12. $CF_3OCF_2CFBrO^{\cdot} \rightarrow CF_3OCF_2C(O)F + Br^{\cdot}$
13. $Br^{\cdot} + CF_2CFBr \rightarrow CF_2BrCFBr^{\cdot}$
14. $CF_2BrCFBr^{\cdot} + O_2 + M \rightarrow CF_2BrCFBrO_2^{\cdot} + M$
15. $2CF_2BrCFBrO_2^{\cdot} \rightarrow 2CF_2BrCFBrO^{\cdot} + O_2$
16. $CF_2BrCFBrO_2^{\cdot} + CF_2CFBr \rightarrow CF_2BrCFBrO_2CF_2CFBr^{\cdot}$
17. $CF_2BrCFBrO_2CF_2CFBr^{\cdot} \rightarrow CF_2BrCFBrO^{\cdot} +$ 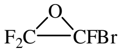 $F_2C\overset{O}{\frown}CFBr$
18. $CF_2BrCFBrO^{\cdot} \rightarrow CF_2BrC(O)F + Br^{\cdot}$
19. $CF_2BrCFBrO^{\cdot} \rightarrow CF_2Br^{\cdot} + C(O)FBr$
20. $CF_2Br^{\cdot} + O_2 + M \rightarrow CF_2BrO_2^{\cdot} + M$
21. $2CF_2BrO_2^{\cdot} \rightarrow 2CF_2BrO^{\cdot} + O_2$
22. $CF_2BrO^{\cdot} \rightarrow C(O)F_2 + Br^{\cdot}$

The formation of traces of bromotrifluoroethene epoxide indicates that small amounts of peroxy radicals $CF_2BrCFBrO_2^{\cdot}$ add to the double bond of CF_2CFBr, regenerating $CF_2BrCFBrO^{\cdot}$. The epoxidation of alkenes by addition of peroxy radical RO_2 to the double bond, producing $RO^{\cdot}$ radical and epoxide, was reported [19].

In presence of NO_2 some peroxy radicals react through the following reaction:

23. $CF_2BrCFBrO_2^{\cdot} + NO_2 \rightarrow CF_2BrCFBrO_2NO_2$

After all the alkene has been consumed in the reaction system $NO_2 + CF_2CFBr + O_2$, the formed $CF_2BrCFBrO_2NO_2$ decomposed slowly to give $CF_2BrC(O)F$, Br_2, $C(O)F_2$, $C(O)FBr$ and NO_2.

The lack of formation of CF_3OOCF_3 indicates that the addition of $CF_3O^{\cdot}$ radicals to the double bond is considerably faster than any other reaction of these radicals.

The respective formations of $O_2NCF_2C(O)F$ and $CF_3C(O)F$ in the corresponding reactions were not detected, showing that, in comparison to the chain products, only very small amounts of these products were formed.

4. Theoretical calculations

A potential energy scan with the B3LYP/6-31 + G* theoretical approximation was performed along the Br–C–C–F torsional angle of $CF_2BrC(O)F$ in order to localize the structures that correspond to the energy minima. All the geometrical parameters were simultaneously relaxed during the calculations while the Br–C–C–F torsional angle was varied in steps of 10°. The resulted potential energy curve depicted in Fig. 1 shows three energy minima. Two of them correspond to equivalent *gauche* structures with τBrCCF equal to +80° and −80°, respectively. The third minimum is localized for a torsional angle of 180° (*anti* conformer). The *syn* form (Br atom *syn* with respect to F atom) constitutes a maximum in the potential energy curve. The energy of each form was then calculated with different approximations with the simultaneous relaxation of all the geometrical parameters. The results, presented in Table 1, show that the *gauche* conformer is the most stable one, according to all the performed calculations. The theoretical proportions of both forms were also obtained from the calculated free energy difference, taking into account the multiplicity of each conformer (m*gauche* = 2 and m*trans* = 1).

Table 2 lists the geometrical parameters of the most stable *gauche* form of $CF_2BrC(O)F$ calculated with different methods. Numbering in the table is in accordance with the structure presented in Fig. 2.

The vibrational spectra of both forms of $CF_2BrC(O)F$ were firstly calculated in order to characterize them as true minima, for which no imaginary frequencies occur. The wavenumbers of the *gauche* and *trans* conformers, together with the IR relative absorption coefficient, are listed in Table 3. From the calculated spectra of both forms we can expect some differences in the spectra due to the different conformers. For example ν_3, assigned to the

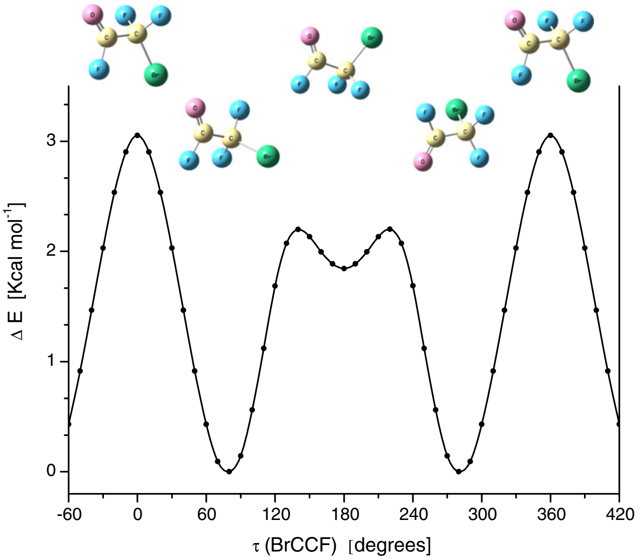

Fig. 1. Potential energy curve for the internal rotation around the C–C single bond of $CF_2BrC(O)F$ at the B3LYP/6-31 + G* level.

Table 1
Calculated energy, energy difference, free energy difference and proportion of the *gauche* and *trans* conformers of $CF_2BrC(O)F$ with different approximation levels[a]

Theoretical method	E *gauche* [hartrees]	E *trans* [hartrees]	ΔE [kcal mol^{-1}]	ΔG [kcal mol^{-1}]	% *gauche*	% *trans*
HF/6-31 + G*	−3018.787557	−3018.783706	2.42	1.65	97	3
B3LYP/6-31 + G*	−3022.659941	−3022.657073	1.80	1.46	96	4

[a] $m_{gauche} = 2$ and $m_{trans} = 1$.

Table 2
Calculated geometrical parameters (distances in Å and angles in degrees) of the *gauche* form of $CF_2BrC(O)F$ with different approximation levels

Geometrical parameter	HF/6-31 + G*	B3LYP/6-31 + G*	MP2/6-31 + G*
C1O	1.161	1.184	1.194
C2C1	1.528	1.538	1.531
BrC2	1.916	1.947	1.928
F2C2	1.314	1.342	1.349
F3C2	1.322	1.349	1.356
F1C1	1.308	1.346	1.354
C2C1O	125.5	126.1	126.3
BrC2C1	109.8	108.9	109.3
F2C2C1	109.2	109.3	109.1
F3C2C1	109.6	110.5	110.1
F1C1C2	110.5	110.1	109.5
F1C1O	124.1	123.8	124.2
F2C2C1O	86.9	87.3	86.8
F3C2C1O	125.1	126.6	125.6
BrC2C1O	103.5	101.3	103.0
BrC2C1F1	75.6	77.5	75.5

Table 3
Wavenumbers and IR relative absorption coefficients of the *gauche* and *anti* forms of $CF_2BrC(O)F$ calculated with different approximation levels

	HF/6-31 + G*		B3LYP/6-31 + G*	
	gauche	*anti*	*gauche*	*anti*
ν_1	1934 (100)	1934 (70)	1935 (100)	1940 (53)
ν_2	1303 (37)	1298 (78)	1257 (46)	1244 (70)
ν_3	1224 (69)	1173 (55)	1176 (90)	1115 (55)
ν_4	1122 (85)	1120 (30)	1090 (98)	1082 (22)
ν_5	950 (53)	968 (100)	915 (62)	942 (100)
ν_6	770 (6)	771 (9)	758 (5)	755 (6)
ν_7	669 (31)	724 (21)	656 (30)	719 (15)
ν_8	584 (8)	617 (6)	581 (10)	616 (4)
ν_9	503 (2)	419 (<1)	505 (3)	417 (<1)
ν_{10}	368 (<1)	332 (<1)	370 (1)	331 (<1)
ν_{11}	324 (<1)	320 (1)	319 (<1)	319 (<1)
ν_{12}	289 (<1)	309 (<1)	286 (<1)	311 (<1)
ν_{13}	238 (<1)	247 (2)	239 (1)	244 (1)
ν_{14}	150 (<1)	164 (<1)	150 (<1)	165 (<1)
ν_{15}	60 (<1)	43 (<1)	59 (<1)	32 (<1)

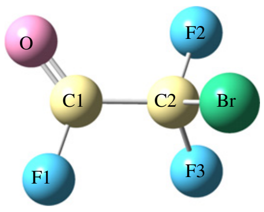

Fig. 2. Atom numbering for $CF_2BrC(O)F$.

antisymmetric stretching vibration of the CF_2 group, is predicted to shift between 50 and 60 cm^{-1} to lower wavenumbers when the *gauche* form is transformed into the *anti* one.

5. Gas phase and matrix-isolated FTIR spectra

Table 4 lists the wavenumbers and relative intensities of the FTIR absorptions of $CF_2BrC(O)F$ in the gas phase and also as isolated in Ar and N_2 matrices, in a proportion ca. 1:1000, together with a tentative assignment of the vibrational modes. Comparing the experimental spectra with those theoretically predicted, we can conclude that only the *gauche* more stable form is present at ambient temperature. Fig. 3 depicts the experimental FTIR spectrum of the gas phase of $CF_2BrC(O)F$ (Pressure 10 Torr, 10 cm path length, 0.5 cm^{-1} resolution) and the IR spectrum simulated with the B3LYP/631 + G* approximation. The agreement between the two spectra is very good.

The assignment of the vibrational absorptions was made by the comparison with related molecules and also with the results obtained from the theoretical calculations. The descriptions of the modes presented here are only approximate, being some of the vibrations mixed together. The band occurring at 1887 cm^{-1} in the gas $CF_2BrC(O)F$ is readily assigned to the C═O vibrational stretching. An overtone of this mode is observed at 3747 cm^{-1}. The absorption at 1265 cm^{-1} is assigned to the C–C stretching; this value is very close to the 1275 cm^{-1} reported for the $CF_2ClC(O)F$ [1] related molecule. The antisymmetric and symmetric stretching of the CF_2 group is assigned to the 1195 and 1102 cm^{-1}, respectively. These modes appear at 1194 and 1107 cm^{-1} in the IR spectrum of $CF_2ClC(O)F$ [1]. The 937 cm^{-1} band is attributable to the C–F stretching mode, in comparison with the 970 cm^{-1} absorption assigned to the same vibrational mode in $CF_2ClC(O)F$ [1]. The bands at 766 and 675 cm^{-1} are assigned to the wagging and deformation of the FCO group, also in accordance with the 768 and 692 cm^{-1} modes of $CF_2ClC(O)F$ [1]. The deformation and rocking vibrations involving the CF_2 group are attributable to the 599 and 503 cm^{-1} absorptions, that correlate very well with the 622 and 518 cm^{-1} bands for $CF_2ClC(O)F$ [1].

There is no sign of the presence of the second conformer either in FTIR spectrum of the gas phase or in the matrix-isolated spectra. Moreover, the irradiation of the matrix with UV–visible Broad-Band light, that is known to pro-

Table 4
Experimental IR wavenumbers and relative intensities of $CF_2BrC(O)F$ in gas phase and isolated in Ar and N_2 matrices

Gas	Ar-matrix	N_2-matrix	Assignment
3747 (<1)	3756.4 (<1)	3747.1 (<1)	2ν (C=O)
1887 (63)	1883.4 1882.6 1880.8 1879.5 (88)	1884.3 1883.4 1882.5 (75)	ν (C=O)
1265 (43)	1267.4 (44)	1267.9 (100)	ν (C–C)
1195 (90)	1191.8 1191.2 (100)	1191.5 1189.2 (88)	ν_{as} (C–F_2)
1102 (100)	1100.6 1099.9 1099.6 1097.6 (86)	1102.9 1100.2 1099.1 1098.4 1097.4 (75)	ν_s (C–F_2)
	980.8 980.4 979.8 (8)	980.4 980.1 979.3 (3)	?
937 (63)	933.3 932.6 931.6 931.2 (53)	932.9 929.4 (53)	ν (C–F)
766 (3)	765.1 (6)	765.4 764.7 (6)	FCO wag
675 (15)	663.8 663.5 661.9 (5)	662.3 662.0 (20)	δ (FCO)
599 (<1)	596.4 (<1)	596.2 (<1)	δ (CF_2)
503 (1)	513.2 507.7 507.4 (< 1)	514.1 513.8 509.4 (< 1)	ρ (CF_2)

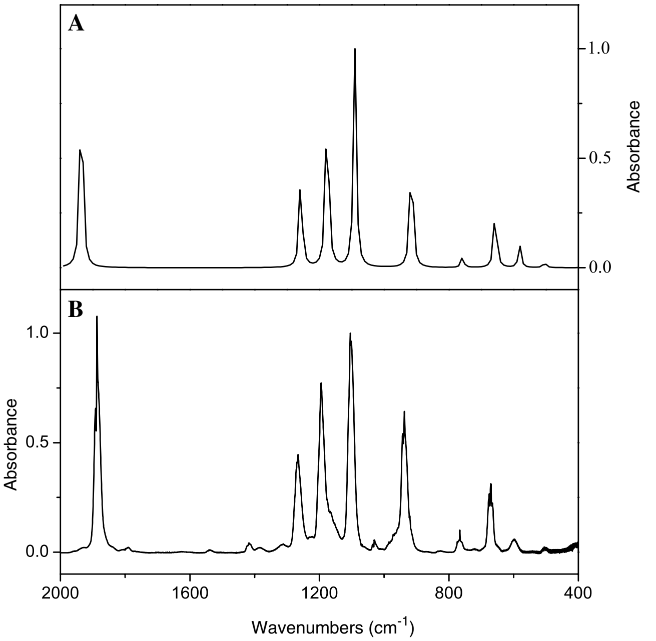

Fig. 3. Comparison of the simulated IR spectrum for the *gauche* conformer of $CF_2BrC(O)F$ using the B3LYP/6-31 + G* approximation (A) with the gas phase FTIR spectrum (Pressure 10 Torr, 10 cm path length, 0.5 cm^{-1} resolution) (B).

duce the interconversion between different conformers [20,21], had no effect on the features of the FTIR spectra.

6. Conclusions

The theoretical calculations predict the *gauche* form of $CF_2BrC(O)F$ as the most stable one, with an energy difference ca. 2 kcal mol^{-1}. This energy difference means that, from a theoretical point of view, the most stable *gauche* conformer contributes with more than 95% at ambient temperature. This theoretical prediction was experimentally confirmed since the gas phase and matrix-isolated FTIR spectra of $CF_2BrC(O)F$ were fully explained through the presence of the *gauche* form as the only one present in the gas phase at ambient temperatures.

Acknowledgements

The authors thank Mr. Z. Czarnowski for helpful comments. This work was supported by the Consejo Nacional de Investigaciones Científicas y Técnicas, CONICET. R.M.R. thanks Fundación Antorchas (14022-3), CONICET (PEI-6177) and Volkswagen Foundation (Professors Oberhammer and Della Védova grant) for the purchase of the FTIR instrument.

References

[1] B.R. Drew, T.K. Gounev, G.A. Guirgis, J.R. Durig, J. Raman Spectrosc. 29 (3) (1998) 205–214.

[2] J.R. Durig, J.F. Davis, G.A. Guirgis, J. Mol. Struct. 328 (1–3) (1994) 19–35.
[3] T.A. Mohamed, H.D. Stidham, G.A. Guirgis, H.V. Phan, J.R. Durig, J. Raman Spectrosc. 24 (1993) 1–10.
[4] V. Arce, M. dos Santos Afonso, R.M. Romano, J. Czarnowski, J. Argentine Chem. Soc. (in press).
[5] F.A. Hohorts, J.M. Shreeve, Inorg. Synth. 11 (1967) 143–146.
[6] P.J.H. Woltz, A.H. Nielsen, J. Chem. Phys. 20 (1952) 307–312.
[7] J.R. Nielsen, C.M. Richards, H.L. McMurry, J. Chem. Phys. 16 (1948) 73–76.
[8] M.J. Almond, A.J. Downs, Adv. Spectrosc. 17 (1989) 1;
I.R. Dunkin, Matrix-Isolation Techniques: A Practical Approach, Oxford University Press, New York, 1998.
[9] R.N. Perutz, J. Turner, J. Chem. Soc., Faraday Trans. 2 69 (1973) 452–461.
[10] M.J. Frisch, G.W. Trucks, H.B. Schlegel, G.E. Scuseria, M.A. Robb, J.R. Cheeseman, V.G. Zakrzewski, J.A. Montgomery Jr., R.E. Stratmann, J.C. Burant, S. Dapprich, J.M. Millam, A.D. Daniels, K.N. Kudin, M.C. Strain, O. Farkas, J. Tomasi, V. Barone, M. Cossi, R. Cammi, B. Mennucci, C. Pomelli, C. Adamo, S. Clifford, J. Ochterski, G.A. Petersson, P.Y. Ayala, Q. Cui, K. Morokuma, D.K. Malick, A.D. Rabuck, K. Raghavachari, J.B. Foresman, J. Cioslowski, J.V. Ortiz, A.G. Baboul, B.B. Stefanov, G. Liu, A. Liashenko, P. Piskorz, I. Komaromi, R. Gomperts, R.L. Martin, D.J. Fox, T. Keith, M.A. Al-Laham, C.Y. Peng, A. Nanayakkara, C. Gonzales, M. Challacombe, P.M.W. Gill, B. Johnson, W. Chen, M.W. Wong, J.L. Andres, M. Head-Gordon, E.S. Replogle, J.A. Pople, Gaussian 98, Revision A.7, Gaussian, Inc., Pittsburgh, PA, 1998.
[11] A.H. Nielsen, T.G. Burke, P.J.W. Woltz, E.A. Jones, J. Phys. Chem. 20 (1952) 596–604.
[12] M.J. Parkington, T.A. Ryan, K.R. Seddon, J. Chem.Soc., Dalton Trans. (1997) 251–256.
[13] P. García, H. Willner, H. Oberhammer, J.S. Francisco, J. Chem. Phys. 121 (2004) 11900–11906.
[14] D. Chow, M.H. Jones, M.P. Thorne, E.C. Wong, Can. J. Chem. 47 (1969) 2491–2494.
[15] R.M. Romano, J. Czarnowski, Z. Phys. Chem. 218 (2004) 575–597.
[16] C.J. Schack, K.O. Christe, J. Fluor. Chem. 14 (1979) 519–522.
[17] J.R. Durig, D.W. Wertz, J. Mol. Spectrosc. 25 (1968) 467–478.
[18] K.R. Loos, R.C. Lord, Spectrochim. Acta 21 (1965) 119–125.
[19] M.S. Stark, J. Phys. Chem. 101 (1997) 8296–8301.
[20] R.M. Romano, C.O. Della Védova, A.J. Downs, T.M. Greene, J. Am. Chem. Soc. 123 (2001) 5794–5801.
[21] R.M. Romano, C.O. Della Védova, A.J. Downs, J. Phys. Chem. A 108 (2004) 7179–7187.